A STRUCTURE-BASED APPROACH FOR TOPOLOGICAL RESOLUTION OF COHERENT TURBULENCE: OVERVIEW AND DEMONSTRATION

Giancarlo Lenci, Emilio Baglietto
Department of Nuclear Science and Engineering
Massachusetts Institute of Technology
77 Massachusetts Avenue, Cambridge, MA 02139, USA
lenci@mit.edu, emiliob@mit.edu

ABSTRACT

Turbulence modeling still represents the weakest link in most computational fluid dynamics (CFD) simulations of unsteady engineering flows. In most cases, the high Reynolds number, dominant presence of wall boundaries, and complex geometrical configurations make the computational cost of Large-Eddy Simulation (LES) prohibitive. Unsteady Reynolds Averaged Navier-Stokes (URANS) models are therefore strongly used today for those applications, albeit unable to provide a complete physical description in regions dominated by high flow deformation. In those regions, the scale separation assumption of URANS models typically loses its validity. URANS/LES hybrid models aim at overcoming the weaknesses of URANS, with the goal of maximizing accuracy for a given grid size. Many of the available hybrid models have shown accurate predictions on a limited number of test cases. Nevertheless, they often exhibit low robustness in internal flow applications and lack of grid consistency, and cannot be relied upon universally. Here, we introduce a new hybrid turbulence approach, which triggers controlled resolution of turbulence inside selected flow regions. The resolution is controlled by a locally varying function of single-point coordinate-invariant parameters, which quantitatively identifies topological flow structures of interest. The model is evaluated here with an a posteriori selection of the closure coefficients, in order to demonstrate the soundness of the concept separately from the dynamic coefficient evaluation. Results of simulations on demanding test cases show, on coarse URANS-like grids, a consistent improvement in the prediction of velocity profiles and normal stresses with respect to URANS. A robust behavior is observed comparable to that of URANS, while significant reduction in computational cost is achieved over LES.

KEYWORDS
Turbulence modeling, Hybrid URANS/LES, STRUCT, NLEVM, Coherent structures

1. INTRODUCTION

Computation of turbulent flows in engineering applications often involves challenging geometries, abundant wall boundaries, and high Reynolds number. This is the case, for example, when simulating nuclear reactor systems. In computational fluid dynamics (CFD) simulations of this kind, turbulence modeling typically represents the largest contributor to the overall prediction error. Industrial simulations nowadays are capable of pushing the boundaries of computational resources, aiming at producing the most accurate flow description while remaining below the threshold of practical feasibility in terms of computational cost. Economic benefits of improved turbulence modeling in industry derive from the reduced need for experimental testing, and from the system efficiency increase made possible by improved optimization capabilities.

In the context of turbulence approaches, a classification can be introduced based on the ratio of total versus unresolved turbulence kinetic energy. In a direct numerical simulation (DNS), all turbulence is resolved, while in Reynolds-averaged Navier-Stokes (RANS) all is modeled. In between DNS and RANS there are, ordered from the most to the least resolved, large-eddy simulation (LES) and unsteady RANS (URANS). Here, we focus on time-dependent simulations, so we shall only refer to URANS instead of RANS.

Computational requirements increase dramatically in the spectrum between URANS and DNS. The CPU requirements for LES are still impracticable for most industrial CFD applications. While it has been estimated that an LES simulation of an airliner wing requires about 10^{20} floating point operations [1], a full reactor core computation would add a few orders of magnitude. Those extreme requirements are related to the coupled constraints on spatial mesh and time discretization, which are especially severe in near-wall regions for wall-resolved cases.

Single-point one or two-equation URANS, being robust and low-cost models, are still widely used in engineering, albeit their well-known lack of accuracy in predicting mean parameters in complex flows. Furthermore, the lack of description of turbulent structures severely limits the capability of URANS to provide useful information on velocity and temperature frequency spectra, which is essential in many applications, including those involving acoustics and fluid-structure interaction (FSI). This category of applications in the nuclear engineering field includes prediction of numerous failure mechanisms, such as vibration-induced fretting or fatigue, and thermal fatigue. URANS models are suitable for high-Re simple flows with nearly homogeneous characteristics [2]. Nevertheless, many engineering applications require simulations of more complex flows.

While no turbulence closure is generally accepted as universal and optimal, the need for improvement over the current models is globally addressed by consistent efforts. Hybrid URANS/LES turbulence models were introduced in the last two decades with the goal of combining the robustness and low cost of URANS, and the augmented flow description of highly resolved models. A good review of hybrid models is provided by Fröhlich and Von Terzi [3].

Two important hybrid models, among the first ones to be developed, are the very large-eddy simulation (VLES) proposed by Speziale [4], and the detached-eddy simulation (DES), proposed by Spalart and co-workers [1] and later improved with more refined variants, mainly to address shortcomings in the near-wall region [5]. The VLES approach of Speziale aims at providing a unique model that should behave as a DNS, LES or URANS based on the computational grid size. The model computes residual stresses by blending URANS and LES based on the ratio of grid size and Kolmogorov length scale. On the other hand, DES, which has been designed specifically for external flows, aims at overcoming the fine-mesh requirement of LES close to the wall by solving URANS equations in attached boundary regions and transitioning to an LES-like model in massively separated regions. Several other models of this kind have been proposed, and can be considered as more complex variants of wall-modeled LES.

After the introduction of VLES and DES, a high number of hybrid turbulence models has been proposed. Two of those are the partially averaged Navier-Stokes (PANS) by Girimaji and co-workers [6], and the scale-adaptive simulation (SAS) by Menter and co-workers [7][8]. In PANS, the goal is to bridge the gap between DNS, LES and URANS by prescribing, a-priori, the desired level of resolution. SAS is a complete hybrid closure that automatically controls the level of turbulence resolution based on the local length scales. Among the many other hybrid models, a few are worthwhile mentioning for the valuable theoretical contribution rather than demonstrated robustness and universal applicability: limited numerical scales (LNS) [9], partially integrated transport model (PITM) [10], partially resolved numerical simulation (PRNS) [11], organized-eddy simulation (OES) [12], temporal partially integrated transport model (TPITM) [13].

In general, hybrid models have shown increased accuracy in specific test cases. However, in practical applications, when non-perfect meshes are adopted, or mixed flow configurations are encountered, existing hybrid models have shown to often produce unacceptably large errors, significantly higher than those of URANS closures [14][15][16]. Most importantly, lack of grid convergence has been observed in complex flow cases. Therefore, those models are practically unworkable for high cost/risk engineering applications.

Aiming at addressing the issues discussed above, we propose a different hybrid approach. This new approach focuses on leveraging the robustness and computational efficiency of URANS in nearly homogeneous regions of the flow, while eliminating its limitations in regions where the assumptions of URANS are not met. In this work, we focus on describing the physical reasoning behind the idea, demonstrating its potential with an a posteriori selection of its closure coefficients.

Analogously to SAS and PANS, the approach modifies the URANS equations without solving the filtered LES ones. Conversely, it is not based on length scales (e.g. SAS), or on scaling coefficients (e.g. PANS). Rather, it partially resolves the energy scales of turbulence inside specific structures, identified based on a comparison between time scales of resolved and residual turbulence. The relation adopted for resolved time scales shares significant similarities with methods used in the literature to identify coherent structures.

The structure-based resolution approach (referred to as STRUCT) is therefore the key element of the closure hereby shown. Its soundness is evaluated over three challenging test cases. The goal of those tests is to evaluate the capabilities of the approach, with emphasis on robustness, efficiency and general applicability. The baseline URANS equations chosen in the tests are those of a robust nonlinear eddy-viscosity k-ε model, in order to provide an advanced flow description in the full domain.

As mentioned, the STRUCT approach is applied here with a posteriori, case-dependent, model parameters, in order to carefully evaluate the method rather than its specific dynamic coefficient implementation. The physical meaning of those parameters and the rationale followed to assign their value are described. This is done to allow for effective discussion, and to stress that the STRUCT philosophy introduced is more general than a specific closure proposal.

Tests performed in this work have shown improved accuracy over URANS on computational grids significantly coarser than those required for LES. Savings in computational cost of 20 to 80 times have been observed over LES. The model has shown to possess grid-convergence capability and low sensitivity to mesh topology. Given these encouraging results, additional work is ongoing to further assess the model's robustness, to identify and address its limitations, and to research areas of improvement. Being a recently developed approach, guidelines on the general use of STRUCT are not yet available and need to be defined. Ultimately, the approach does not aim at substituting the performance of LES for suitable fine meshes, or at retrieving an LES solution in the fine-mesh limit, as some other hybrid models aim at doing.

2. MODEL EQUATIONS

2.1. Similarity between URANS and LES Equations

Albeit deriving from different mathematical theory, most URANS and LES models share the same unclosed equations for resolved momentum and mass conservation [17]. Such similarity is one of the reasons why many hybrid URANS/LES models adopt closures based on simple variations of the original equations.

As remarked by Perot and Gadebusch [18], the URANS and LES unclosed equations could be derived solely based on the assumption that the statistical operation involved commutes with differentiation. Such operation will be marked with an overbar, which has a different meaning in URANS and LES. It denotes ensemble averaging in URANS, and spatial filtering by convolution of the velocity and pressure fields with a commuting filter function in many LES formulations [19]. The expression in (1) is obtained by applying such operation to the incompressible equations for momentum and mass conservation.

$$\frac{\partial \bar{u}_i}{\partial t} + \bar{u}_j \frac{\partial \bar{u}_i}{\partial x_j} = -\frac{1}{\rho}\frac{\partial \bar{p}}{\partial x_i} + \nu \frac{\partial^2 \bar{u}_i}{\partial x_j \partial x_j} - \frac{\partial \tau_{ij}}{\partial x_j}, \quad \frac{\partial \bar{u}_j}{\partial x_j} = 0 \tag{1}$$

Provided this similarity between the two approaches, here we use the term resolved to refer to fields such as $\bar{u}_i$ and $\bar{p}$. In a steady flow case, the instantaneous velocity can be split in a triple decomposition as in (2). The time average of resolved velocity is defined as $\hat{u}_i$, and a residual resolved component as $\tilde{u}_i = \bar{u}_i - \hat{u}_i$. Deviation with respect to the time average is $u_i' = u_i - \hat{u}_i$.

$$u_i = \hat{u}_i + \tilde{u}_i + u_i'' \tag{2}$$

Parameter u_i'' in (2) is the residual velocity, defined as $u_i'' = u_i - \bar{u}_i$. The same decomposition applies to the pressure term. Momentum transfer between resolved and residual velocity is taken into account by a residual stress tensor, describing transfer of momentum into the resolved flow due to acceleration in the residual velocity field:

$$\tau_{ij} = \overline{u_i u_j} - \bar{u}_i \bar{u}_j \tag{3}$$

In URANS, properties of the ensemble averaging operation lead to decomposition of velocity into a random and a non-random part. Consequently, through basic algebra [20] the residual stress tensor can be more simply expressed as the covariance of the residual fluctuations $\tau_{ij} = \overline{u_i'' u_j''}$. In LES, resolved variables have a randomly fluctuating nature, so the aforementioned expression is not valid unless additional assumptions are made. In URANS and LES, τ_{ij} is often modeled using the Boussinesq approximation, which relates the anisotropic part of residual stresses a_{ij} to the resolved rate of strain $\bar{S}_{ij}$, through the eddy viscosity ν_t.

$$a_{ij} = \tau_{ij} - \frac{2}{3} k \delta_{ij} = -2\nu_t \bar{S}_{ij} \tag{4}$$

The residual turbulence kinetic energy is defined as: $k = \tau_{ii}/2$. The resolved rate of strain and rate of rotation tensors are:

$$\bar{S}_{ij} = \frac{1}{2}\left(\frac{\partial \bar{u}_i}{\partial x_j} + \frac{\partial \bar{u}_j}{\partial x_i}\right) \quad , \quad \bar{\Omega}_{ij} = \frac{1}{2}\left(\frac{\partial \bar{u}_i}{\partial x_j} - \frac{\partial \bar{u}_j}{\partial x_i}\right) \tag{5}$$

In the well-known Smagorinsky LES model [21], the eddy viscosity ν_t is expressed in a form similar to mixing length models as the product between a term containing grid size, Δ, and a parameter defined based on the resolved rate of strain, as: $\bar{S} = \left(2\bar{S}_{ij}\bar{S}_{ij}\right)^{1/2}$.

$$\nu_t = (C_s \, \Delta)^2 \bar{S} \tag{6}$$

Where the C_s coefficient is undesirably dependent on the flow case. In the standard k-ε closure [22], ν_t is calculated based on two transported turbulence parameters: the turbulence kinetic energy k and turbulence dissipation rate ε.

$$\nu_t = C_\mu \frac{k^2}{\varepsilon} \tag{7}$$

2.2. Cubic URANS Equations

Linear eddy-viscosity models present a linear relation between residual stress anisotropy and resolved rate of strain. Due to such assumption, effects of residual turbulence on the resolved flow are oversimplified. This leads to gross overestimate of turbulent viscosity in complex strains, and lack of description of some unsteady flow features, which would plague the full effectiveness of hybrid formulations. In this work, in order to overcome this limitation, a nonlinear formulation as proposed by Pope [2] is adopted. This choice allows us to capture the effects of asymmetry and anisotropy in the relation for residual stresses, thus allowing for a more complete description of large-scale phenomena, e.g. vortex stretching. Anisotropic stresses are expressed through a coordinate-invariant polynomial function of k, ε, and the resolved velocity gradient tensor. Such approach is referred to as nonlinear eddy-viscosity model (NLEVM), and multiple variants exist in the literature.

The cubic NLEVM closure proposed by Baglietto and Ninokata [23][24] is selected. Their model is based on the original proposal of Shih, Zhu and Lumley [25], where they reformulated the model coefficients on the base of their physical interpretation, leveraging DNS data, to extend the generality of the formulation. The residual stress anisotropy tensor expands the linear formulation by adding quadratic and cubic terms.

$$a_{ij} = \tau_{ij} - \frac{2}{3}k\delta_{ij} = -2\nu_t\bar{S}_{ij} + q_{ij} + c_{ij} \tag{8}$$

Those two additional terms are:

$$\begin{gathered} q_{ij} = 4C_1\nu_t\frac{k}{\varepsilon}\left[\bar{S}_{ik}\bar{S}_{kj} - \frac{1}{3}\delta_{ij}\bar{S}_{kl}\bar{S}_{kl}\right] + 4C_2\nu_t\frac{k}{\varepsilon}\left[\bar{\Omega}_{ik}\bar{S}_{kj} + \bar{\Omega}_{jk}\bar{S}_{ki}\right] \\ +4C_3\nu_t\frac{k}{\varepsilon}\left[\bar{\Omega}_{ik}\bar{\Omega}_{jk} - \frac{1}{3}\delta_{ij}\bar{\Omega}_{kl}\bar{\Omega}_{kl}\right] \end{gathered} \tag{9}$$

$$c_{ij} = 8C_4\nu_t\frac{k^2}{\varepsilon^2}\left[\bar{S}_{ki}\bar{\Omega}_{lj} + \bar{S}_{kj}\bar{\Omega}_{li}\right]\bar{S}_{kl} + 8C_5\nu_t\frac{k^2}{\varepsilon^2}\left[\bar{S}_{kl}\bar{S}_{kl} + \bar{\Omega}_{kl}\bar{\Omega}_{kl}\right]\bar{S}_{ij} \tag{10}$$

Let us define the following dimensionless parameters for the resolved strain and rotation:

$$\bar{S}^* = \frac{k}{\varepsilon}\sqrt{2\bar{S}_{ij}\bar{S}_{ij}} \quad , \quad \bar{\Omega}^* = \frac{k}{\varepsilon}\sqrt{2\bar{\Omega}_{ij}\bar{\Omega}_{ij}} \tag{11}$$

The non-constant coefficients used in (10) are the following. Notice that for C_4 and C_5 the simple form discussed by Lien, Chen and Leschziner has been employed [26].

$$C_\mu = \frac{C_{a0}}{C_{a1} + C_{a2}\bar{S}^* + C_{a3}\bar{\Omega}^*} \tag{12}$$

$$C_1 = \frac{C_{NL1}}{(C_{NL6} + C_{NL7}\bar{S}^{*3})C_\mu} \tag{13}$$

$$C_2 = \frac{C_{NL2}}{(C_{NL6} + C_{NL7}\bar{S}^{*3})C_\mu} \tag{14}$$

$$C_3 = \frac{C_{NL3}}{(C_{NL6} + C_{NL7}\bar{S}^{*3})C_\mu} \tag{15}$$

$$C_4 = C_{NL4}C_\mu^2 \tag{16}$$

$$C_5 = C_{NL5}C_\mu^2 \tag{17}$$

Table I. Cubic NLEVM constants

C_{a0}	C_{a1}	C_{a2}	C_{a3}	C_{NL1}	C_{NL2}	C_{NL3}	C_{NL4}	C_{NL5}	C_{NL6}	C_{NL7}
0.667	3.9	1.0	0.0	0.8	11.0	4.5	-5.0	-4.5	1000.0	1.0

The model constants employed are derived from the work of Baglietto and Ninokata [23], in which coefficients C_{NL4} and C_{NL5} have been calculated in order to match the simpler formulation in (16) and (17) in case of null resolved rotation and strain. Those constants are shown in Table I.

2.3. STRUCT Approach

2.3.1. Rationale and time scales

In his 1975 paper, Pope [2] identified two reasons why isotropic turbulence viscosity models fail at predicting many flows. One is the inadequacy of the isotropic-viscosity hypotheses, and the other is the inapplicability of the effective-viscosity approach. In that paper, he addressed the former limitation by introducing NLEVMs. The latter limitation, i.e. the restriction of URANS to quasi-homogeneous flows, remains a weakness of two-equation URANS models. Here, we address this challenge by proposing a new hybrid approach.

The ensemble average operation is based on the assumption of statistically stationary residual fluctuations. In flows for which this condition is met, scale separation exists between turbulence and slowly varying phenomena, such as a gently varying inlet velocity. Basic URANS models are not meant to be used when residual fluctuations are far from being statistically stationary. This happens, for example, in flows with large-scale anisotropic vortical structures [3], curvature, intermittency, buoyancy, swirl [27]. Such cases are very frequent in engineering applications, in which it is usually not affordable to leverage LES.

The STRUCT approach addresses this challenge in a distinctive way: by using URANS in flow regions where its underlying assumptions are met, and eliminating the URANS inconsistency by partially resolving turbulence in regions with lack of scale separation.

The rationale is known since many decades. For example, rapid distortion theory (RDT), has been applied to predict the short-term response to a strong deformation. Such condition is defined by comparing the resolved deformation time scale with the turbulence time scale. It takes place when $\bar{S}^*$ is much greater than 1 in shear flows, or $\bar{\Omega}^*$ much greater than 1 in rotating flows. In STRUCT, the resolved deformation time scale is defined based on the second invariant of the resolved velocity gradient tensor, which is:

$$\overline{II} = -\frac{1}{2}\frac{\partial \bar{u}_i}{\partial x_j}\frac{\partial \bar{u}_j}{\partial x_i} = \frac{1}{2}(\bar{\Omega}_{mn}\bar{\Omega}_{mn} - \bar{S}_{mn}\bar{S}_{mn}) \tag{18}$$

The frequency associated with resolved turbulence is hereby defined as:

$$f_r = \sqrt{|\overline{II}|} \tag{19}$$

Parameter f_r is used to identify high-deformation regions characterized by either strong strain or rotation.

2.3.2. Basic formulation

The proposed hybrid formulation is triggered by comparison of f_r as defined in (19) with a value representing the characteristic frequency of residual turbulence, $f_{r,0}$.

The most basic formulation of the STRUCT approach is:

$$\nu_t = \begin{cases} \nu_{t,0} & f_r < f_{r,0} \\ \phi \nu_{t,0} & f_r \geq f_{r,0} \end{cases} \tag{20}$$

High-deformation structures are identified as locations where f_r is larger than $f_{r,0}$. Heuristically, we can imagine this to occur in locations with lack of scale separation, where URANS attempts to model eddies that are larger than resolved ones. In such condition, a damping coefficient ϕ is used to reduce the turbulent viscosity $\nu_{t,0}$ calculated as in (7). Application of this damping coefficient reduces the ratio of residual to total turbulence kinetic energy, following an approach similar to other hybrid models (e.g. [18][6]).

In the test cases shown below, parameters $f_{r,0}$ and ϕ are selected a posteriori. This is a choice of the authors, to demonstrate the STRUCT philosophy in its more general formulation. The complete versions of STRUCT require a separate discussion, and will appear in the near future.

The value for $f_{r,0}$ is hereby determined based on a representative value of ε/k obtained from the bulk flow in URANS results.

The damping coefficient ϕ is representative of how much of the total turbulence kinetic energy should be resolved in the selected structures. A robust value equal to 0.6 produced enhanced accuracy over URANS in all the cases tested, and is used here unless otherwise specified. Further local optimization of this parameter is also being evaluated but not discussed here.

The approach presented satisfies the Galilean and frame invariance requirements, since it only involves constant scalars, an invariant, and a closure that already satisfies those requirements. It is a single-point closure, only involving transported turbulence quantities and derivatives of velocity, thus minimizing the computational burden. Calculation time on an equal number of cores has shown through our tests to be about 10-20% higher when the STRUCT approach is adopted, compared to using just URANS.

2.3.3. Additional interpretations

It is interesting to discuss some additional interpretations that have been made for $\overline{II}$. Let us start by defining its instantaneous counterpart:

$$II = -\frac{1}{2}\frac{\partial u_i}{\partial x_j}\frac{\partial u_j}{\partial x_i} \tag{21}$$

This parameter has been used by several authors (e.g. [28]) to identify coherent structures. Such concept is recurring but still scarcely leveraged in turbulence modeling.

According to Hussain [29], turbulence is characterized by quasi-deterministic structures that are randomly distributed in space and time. According to Hunt, Wray and Moin [30], values of II below a certain negative threshold and above a certain positive one are among the requirements to identify respectively regions defined as eddy zones and regions defined as convergence zones. According to Rousseaux et al. [31], vortex cores can be identified as circular regions with positive II around a peak of vorticity. While there is no commonly accepted definition of coherent structure, Robinson [32] provides a useful description:

Three-dimensional region of the flow over which at least one fundamental flow variable (velocity component, density, temperature, etc.) exhibits significant correlation with itself or with another variable over a range of space and/or time that is significantly larger than the smallest local scales of the flow.

Therefore, phase correlation distinguishes coherent structures from other regions of high vorticity. Single-point turbulence models are local by definition, while the phenomenon of turbulence is nonlocal. Phases with different intensities exist such as "bursts" and "lulls". Such an organization suggests that turbulence time averaging is un-natural [33]. Hussain [34] uses a triple decomposition similar to the one in (2), where the statistical operation marked with an overbar is defined as phase average, decomposing velocity into a coherent and incoherent part. This decomposition shares clear similarities with the philosophy of the STRUCT approach.

Formulation of a turbulence model leveraging the concept of coherent structures described by parameter $\overline{II}$ has been already made by Kobayashi [35] in an innovative structure-based LES closure. The same author remarks that it can be demonstrated that II vanishes on non-slip walls. This property, translated to $\overline{II}$, plays an important role in STRUCT. It allows for the hybrid formulation not to trigger its partially resolved capability in the near-wall limit, which is a desirable and common feature of hybrid models.

3. COMPUTATIONAL DETAILS

3.1. Solver and Numerical Schemes

Model testing is performed with the commercially available finite-volume CFD solver, STAR-CCM+ in a modified development version of its release 7.02. A segregated flow solver is used, based on the SIMPLE algorithm and is applied on co-located variables using Rhie-Chow interpolation [36]. Common under-relaxation factors are used, being 0.7 for velocity, 0.3 for pressure and 0.8 for both the turbulent kinetic energy and turbulent dissipation rate [37].

Second-order, three-time-level implicit time integration is used, while convective terms are interpolated by a non-oscillatory second-order upwind scheme for URANS solutions. A locally-bounded central differencing scheme is used to compute convective terms for LES and STRUCT. A hybrid Gauss-least square method is used for computing reconstruction gradients, with the Venkatakrishnan's reconstruction gradient limiter [38]. The time step is selected to enforce that the maximum Courant number remain below 1. Fluids are simulated assuming constant density and molecular viscosity. In general, STRUCT uses the same numerical schemes both in the fully modeled and in the partially resolved regions.

3.2. Test Cases

Three different flow cases are examined to demonstrate the STRUCT approach, representative of practical flow configurations in industrial applications. Validation of the approach on the three test cases is a first step to assess the applicability of the model to complex flows combining multiple phenomena.

3.2.1. Flow past a square cylinder

The flow past a square cylinder test case is representative of external flows, and is useful to test the behavior of turbulence models in massively separated regions. Here, we used the experimental data of Lyn et al. [39], that consider the flow through a channel with a 39 cm x 56 cm cross section. The square cylinder side size is 4 cm, which leads to a Reynolds number of 21,400. Experiments were collected using laser-Doppler velocimetry (LDV) techniques. A structured 10.5 mm mesh was used, refined by 50% in a region around and past the obstacle. A low-Re treatment has been adopted for the walls around the obstacle, while a wall function has been used for top and bottom walls, and periodic boundary conditions have been adopted in the spanwise direction. The inlet boundary has been extruded in order to achieve a fully-developed profile. Using such extruded geometry, the uniform inlet velocity has been selected as 0.5435 m/s to match the upstream experimental profiles. The total size of this mesh is 646,000 cells, on which URANS grid convergence has been tested and achieved.

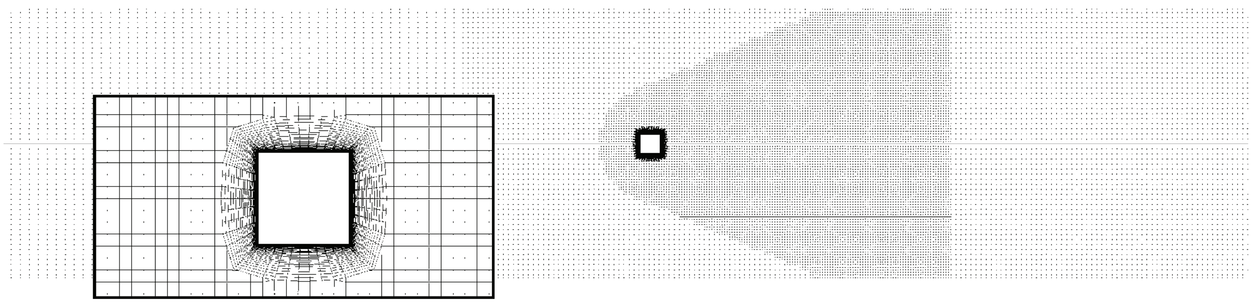

Figure 1. Flow past a square cylinder, computational grid

3.2.2. Turbulent mixing in a T-junction

The T-junction test case is representative of turbulent mixing and of phenomena that can lead to thermal fatigue in structural materials. Water (19 °C) flowing through a 140 mm diameter pipe encounters an intersection where "hot" (36 °C) water is injected through a 100 mm diameter pipe. The two inflowing streams have a volumetric flow rate of $9 \times 10^{-3}\ \mathrm{m^3/s}$ (cold) and $6 \times 10^{-3}\ \mathrm{m^3/s}$ (hot). Experimental acquisitions [16] include LDV and particle-image velocimetry (PIV), and temperature measurements made using thermocouples. A 4.5 mm trimmed mesh has been used in the simulation, and wall functions have been prescribed at all walls. A segregated-fluid-temperature model has been used, and inlet profiles have been taken from the experiment. The size of this URANS-converged computational grid is 746,000 cells.

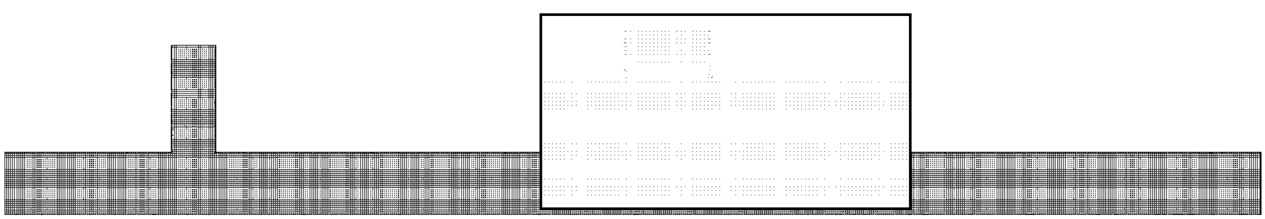

Figure 2. Turbulent mixing in a T-junction, computational grid

3.2.3. Mild separation in an asymmetric diffuser

The asymmetric diffuser test case reproduces the phenomenon of flow separation. Air flows through a 0.515 × 0.015 m rectangular duct. The Reynolds number based on the 0.015 m height of the inlet channel and the bulk inlet velocity is 20,000. In the diffuser section, the bottom wall has a slope with a 10° angle. Experimental data were collected by Buice [40], using hot-wire anemometry. A computational grid has been used with a variable cell size that is roughly 1 mm in the majority of the domain, and refined by the inlet. The size of this grid is 1,800,000 cells. Inlet profiles have been taken from the experiment. Top and bottom boundaries have been treated with low-Re approach, while periodic boundary conditions have been adopted in the spanwise direction.

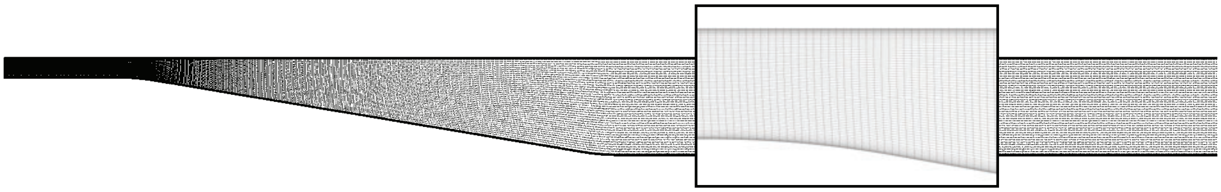

Figure 3. Mild separation in an asymmetric diffuser, computational grid

4. MODEL VALIDATION

4.1. Flow past a Square Cylinder

The flow past a square cylinder is a test case in which several hybrid models have shown accurate results. As an example, PANS [41][42] has shown to provide results closer to the experiment for increased turbulence resolution. This case can be considered trivial for hybrid models, since results obtained without any residual stress are superior to those obtained using any k-ε model, either linear or nonlinear. Accordingly, here a damping coefficient close to zero is selected for optimal predictions: $\phi = 1 \times 10^{-10}$.

Using the guidelines defined in section 2.3.2, we determine the value $f_{r,0} = 3$ Hz. The test allows a simple graphical demonstration of the underlying approach, shown in Figure 4, where the URANS region is shown in red while the hybrid turbulence activation region is shown in blue. In such a clear-cut case it is evident how the model can select the activation regions without the need to depend on length scales or grid sizes. The same figure shows that STRUCT leverages the robustness of URANS in all the undisturbed regions.

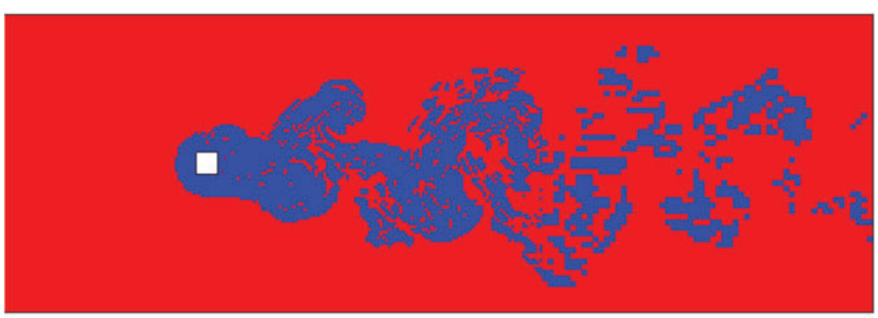

Figure 4. Flow past a square cylinder, regions of STRUCT model activation (in blue)

Velocity profiles in the flow direction are shown in Figure 5. The STRUCT results confirm the expected accuracy improvement in comparison to the underlying NLEVM URANS model. While not shown here, those improvements are consistent on all grid sizes.

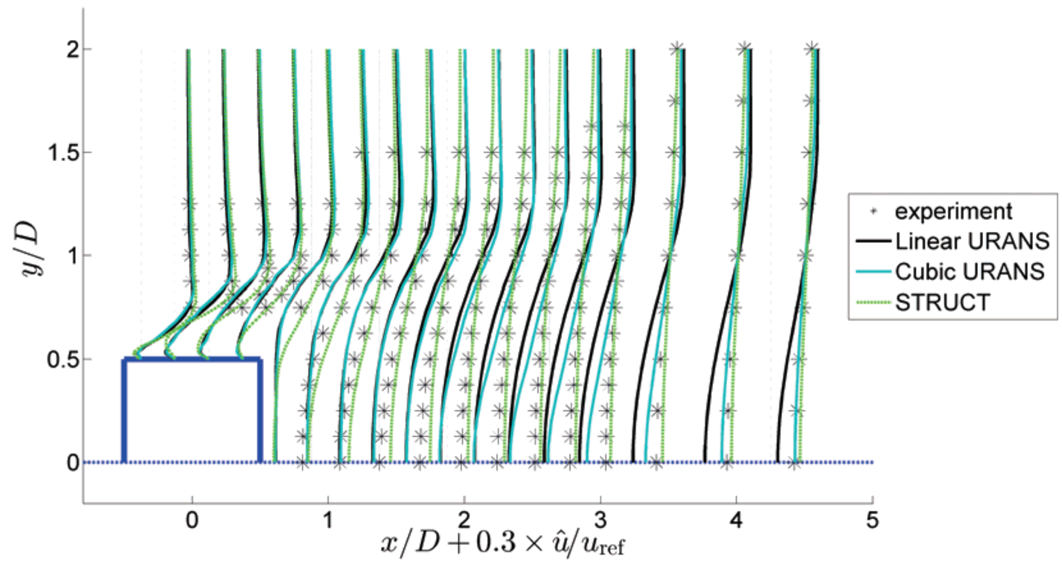

Figure 5. Flow past a square cylinder, velocity profiles

4.2. Turbulent Mixing in a T-Junction

In the T-junction test case, using the guidelines specified in section 2.3.2, we determined that $f_{r,0} = 10$ Hz. The URANS and STRUCT results are compared to the experiment and to an LES simulation run on a mesh about 81 times larger (base size 1.5 mm), necessary to resolve the integral length scales. An example of the results obtained is shown in Figure 6. Velocity profiles predicted by the STRUCT approach match the experiment much more closely than URANS on the same coarse mesh, achieving similar accuracy compared to the fine-mesh LES, at a computational cost lower by two orders of magnitude.

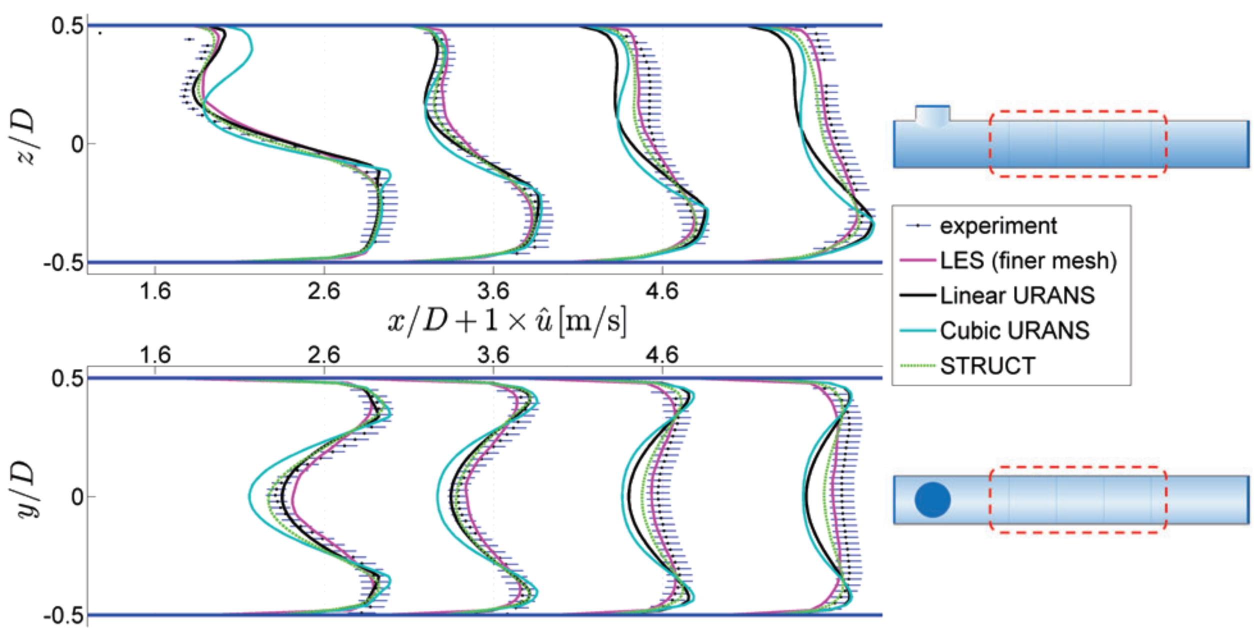

Figure 6. Turbulent mixing in a T-junction, velocity profiles

4.3. Mild Separation in an Asymmetric Diffuser

The asymmetric diffuser case has shown to be a particularly challenging one for hybrid models. In the work of Davidson [14] for example the SAS closure produces wildly inaccurate predictions of velocity profiles and turbulent stresses. STRUCT results for velocity profiles are shown in Figure 7.

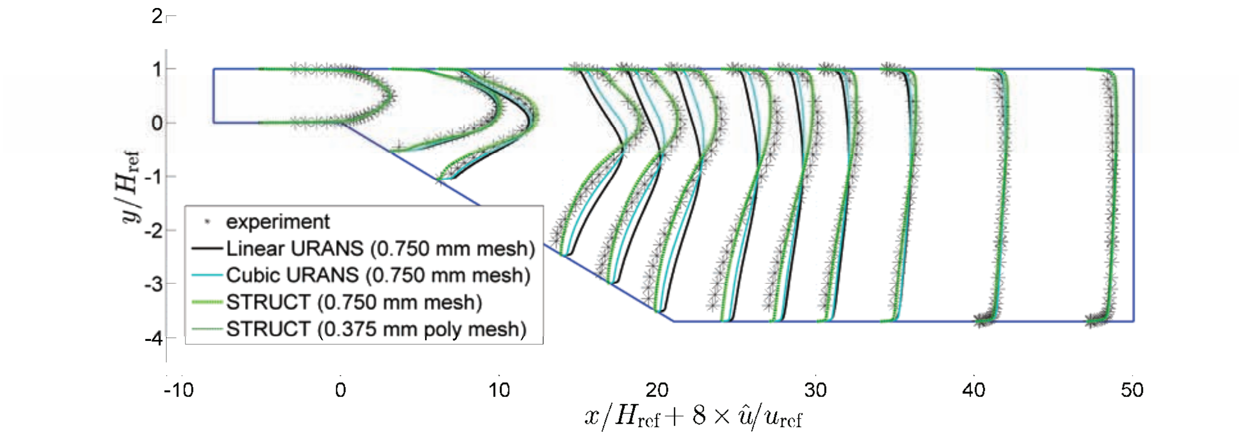

Figure 7. Mild separation in an asymmetric diffuser, velocity profiles

In this test case, we determined using the guidelines specified in section 2.3.2 a value $f_{r,0} = 100$ Hz. In Figure 7, we notice a solution closer to the experiment when switching from linear to cubic URANS, and a much improved agreement when the STRUCT approach is enabled. Figure 7 also shows results obtained with an 8 times larger mesh, demonstrating grid convergence. In the same test, the STRUCT approach has shown to provide basically the same result when switching from a trimmed mesh to a polyhedral mesh of the same base size, thus demonstrating robustness to the mesh type.

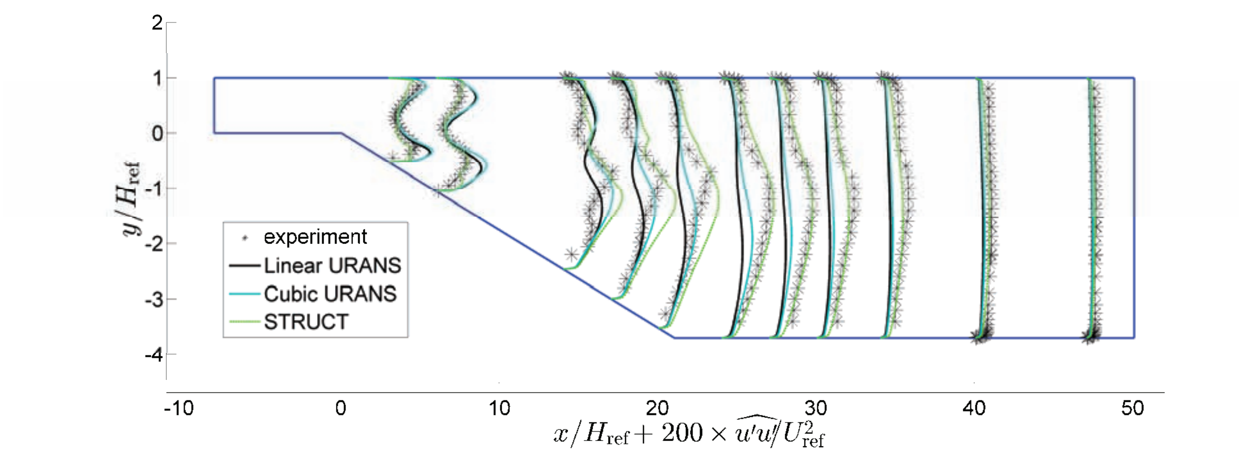

Figure 8. Mild separation in an asymmetric diffuser, velocity variance profiles

Figure 8 shows profiles for velocity variance in the direction of the flow. The STRUCT model provides a more accurate description of those fluctuations compared to linear and cubic URANS.

5. CONCLUSIONS

A new hybrid turbulence approach has been introduced that aims at overcoming the weaknesses of URANS in unsteady engineering simulations. Partial resolution of turbulence is applied in regions where the underlying URANS assumption of scale separation is not met. The topological structures of interest are identified based on comparison between time scales of resolved and residual turbulence.

The model has been evaluated on three demanding flow cases, representative of flow phenomena in engineering applications. An a posteriori selection of the closure coefficients has been made, in order to demonstrate the soundness of the concept separately from the dynamic coefficient evaluation. For all test cases, the new STRUCT approach has demonstrated LES-like capabilities on much coarser grids than those needed for LES. The STRUCT approach has shown to consistently improve the prediction accuracy of the baseline URANS model, and to provide reduction in computational cost of 20 to 80 times.

The encouraging results obtained with the STRUCT approach show its potential to introduce a new class of predictive unsteady simulations. A robust and accurate low-cost turbulence model would allow the capabilities of industrial CFD to be extended to more complex applications.

Ongoing and future work aims at leveraging the promising behavior of the STRUCT approach presented, moving towards an industry-ready model. The ultimate objective is to propose a hybrid approach capable of ensuring robustness while possessing desirable characteristics in all the five criteria identified by Pope for appraising turbulence models: level of description, completeness, cost and ease of use, range of applicability and accuracy.

ACKNOWLEDGMENTS

This project has benefitted from the support of various institutions, including the DOE-sponsored NEAMS project, TerraPower and AREVA.

REFERENCES

[1] P. Spalart, W.-H. Jou, M. K. Strelets, and S. Allmaras, "Comments on the feasibility of LES for wings, and on a hybrid RANS/LES approach," in *Proceedings of the First AFOSR International Conference on DNS/LES, Advances in DNS/LES*, 1997, pp. 137–147.
[2] S. B. Pope, "A more general effective-viscosity hypothesis," *Journal of Fluid Mechanics*, vol. 72, no. 2. pp. 331–340, 1975.
[3] J. Fröhlich and D. von Terzi, "Hybrid LES/RANS methods for the simulation of turbulent flows," *Prog. Aerosp. Sci.*, vol. 44, no. 5, pp. 349–377, 2008.
[4] C. G. Speziale, "Computing non-equilibrium turbulent flows with time-dependent RANS and VLES," in *Proceedings of the 15th International Conference on Numerical Methods in Fluid Dynamics*, 1996, pp. 123–129.
[5] P. R. Spalart, "Detached-Eddy Simulation," *Annual Review of Fluid Mechanics*, vol. 41. pp. 181–202, 2009.
[6] S. S. Girimaji, R. Srinivasan, and E. Jeong, "PANS Turbulence model for seamless transition between RANS and LES: fixed-point analysis and preliminary results," in *Proceedings of the 4th ASME-JSME Joint Fluids Engineering Conference*, 2003, pp. 1–9.
[7] F. R. Menter, M. Kuntz, and R. Bender, "A scale-adaptive simulation model for turbulent flow predictions," in *41st Aerospace Sciences Meeting and Exhibit*, 2003, pp. 1–11.
[8] F. R. Menter and Y. Egorov, "The scale-adaptive simulation method for unsteady turbulent flow predictions. part 1: Theory and model description," *Flow, Turbul. Combust.*, vol. 85, no. 1, pp. 113–138, Jun. 2010.
[9] P. Batten, U. Goldberg, and S. Chakravarthy, "Sub-grid turbulence modeling for unsteady flow with acoustic resonance," in *Proceedings of the 38th Aerospace Sciences Meeting & Exhibit*, 2000, pp. 1–8.
[10] B. Chaouat and R. Schiestel, "Partially integrated transport modeling method for turbulence simulation with variable filters," *Phys. Fluids*, vol. 25, no. 12, pp. 1–39, 2013.
[11] T. Shih and N. Liu, "Assessment of the Partially Resolved Numerical Simulation (PRNS) Approach in the National Combustion Code (NCC) for Turbulent Nonreacting and Reacting Flows," NASA/TM-2008-215418, 2008.

[12] R. Bourguet, M. Braza, G. Harran, and R. El Akoury, "Anisotropic Organised Eddy Simulation for the prediction of non-equilibrium turbulent flows around bodies," *J. Fluids Struct.*, vol. 24, no. 8, pp. 1240–1251, 2008.
[13] A. Fadai-Ghotbi, C. Friess, R. Manceau, T. B. Gatski, and J. Borée, "Temporal filtering: A consistent formalism for seamless hybrid RANS-LES modeling in inhomogeneous turbulence," *Int. J. Heat Fluid Flow*, vol. 31, no. 3, pp. 378–389, 2010.
[14] L. Davidson, "Evaluation of the SST-SAS model: Channel flow, asymmetric diffuser and axi-symmetric hill," in *Proceedings of the European Conference on Computational Fluid Dynamics (ECCOMAS CFD 2006)*, 2006, pp. 1–20.
[15] M. S. Gritskevich, A. V. Garbaruk, T. Frank, and F. R. Menter, "Investigation of the thermal mixing in a T-junction flow with different SRS approaches," *Nuclear Engineering and Design*, vol. 279, pp. 83–90, 2014.
[16] B. L. Smith, J. H. Mahaffy, K. Angele, and J. Westin, "Report of the OECD/NEA-Vattenfall T-Junction Benchmark exercise," NEA/CSNI/R(2011)5, 2011.
[17] M. Germano, "Turbulence - The filtering approach," *J. Fluid Mech.*, vol. 238, pp. 325–336, 1992.
[18] B. J. Perot and J. Gadebusch, "A self-adapting turbulence model for flow simulation at any mesh resolution," *Phys. Fluids*, vol. 19, no. 11, pp. 1–11, 2007.
[19] A. Leonard, "Energy Cascade in large-eddy simulations of turbulent fluid flows," *Adv. Geophys*, vol. 18A, pp. 237–248, 1974.
[20] S. Pope, *Turbulent flows*. Cambridge University Press, 2000.
[21] J. Smagorinsky, "General circulation experiments wiht the primitive equations I. The basic experiment," *Mon. Weather Rev.*, vol. 91, no. 3, pp. 99–164, 1963.
[22] B. Launder and D. Spalding, "The numerical computation of turbulent flows," *Comput. Methods Appl. Mech. Eng.*, vol. 3, no. 2, pp. 269–289, 1974.
[23] E. Baglietto and H. Ninokata, "Anisotropic Eddy Viscosity Modeling for Application to Industrial Engineering Internal Flows," *Int. J. Transp. Phenom.*, vol. 8, no. 2, pp. 85–101, 2006.
[24] E. Baglietto and H. Ninokata, "Improved turbulence modeling for performance evaluation of novel fuel designs," *Nucl. Technol.*, vol. 158, no. 2, pp. 237–248, 2007.
[25] T. Shih, J. Zhu, and J. L. Lumley, "A Realizable Reynolds Stress Algebraic Equation Model," *NASA Technical Memorandum 105993*, pp. 1–34, 1993.
[26] F. Lien, W. Chen, and M. Leschziner, "Low-Reynolds-number eddy-viscosity modelling based on non-linear stress-strain/vorticity relations," in *Proceedings of the 3rd symposium on Engineering turbulence modelling and Experiments*, 1996, vol. 3, pp. 91–100.
[27] C. D. Argyropoulos and N. C. Markatos, "Recent advances on the numerical modelling of turbulent flows," *Appl. Math. Model.*, vol. 39, no. 2, pp. 693–732, 2014.
[28] Y. Dubief and F. Delcayre, "On coherent-vortex identification in turbulence," *Journal of Turbulence*, vol. 1. pp. 1–22, Jan-2000.
[29] A. K. M. F. Hussain, "Coherent structures - Reality and myth," *Phys. Fluids*, vol. 26, no. 10, pp. 2816–2850, 1983.
[30] J. C. R. Hunt, A. A. Wray, and P. Moin, "Eddies, streams, and convergence zones in turbulent flows," in *Center for Turbulence Research, Proceedings of the Summer Program*, 1988, pp. 193–208.
[31] G. Rousseaux, S. Seifer, V. Steinberg, and A. Wiebel, "On the Lamb vector and the hydrodynamic charge," *Exp. Fluids*, vol. 42, no. 2, pp. 291–299, Dec. 2007.
[32] S. K. Robinson, "Coherent motions in the turbulent boundary layer," *Annu. Rev. Fluid Mech.*, vol. 23, pp. 601–639, 1991.
[33] P. R. Spalart, "Philosophies and fallacies in turbulence modeling," *Prog. Aerosp. Sci.*, vol. 74, pp. 1–15, 2015.
[34] A. K. M. F. Hussain, "Coherent structures and turbulence," *J. Fluid Mech.*, vol. 173, pp. 303–356, 1986.
[35] H. Kobayashi, "The subgrid-scale models based on coherent structures for rotating homogeneous turbulence and turbulent channel flow," *Phys. Fluids*, vol. 17, no. 4, pp. 2350–2360, 2005.
[36] W. L. Rhie, C.M and Chow, "Numerical Study of the Turbulent Flow Past an Airfoil with Trailing Edge Separation," *AIAA J.*, vol. 21, no. 11, pp. 1525–1532, 1983.
[37] J. H. Ferziger and M. Peric, *Computational Methods for Fluid Dynamics*. Springer-Verlag Berlin Heidelberg, 2002.
[38] V. Venkatakrishnan, "On the accuracy of limiters and convergence to steady state solutions," in *31st Aerospace Sciences Meeting & Exhibit*, 1993, pp. 1–10.
[39] D. a. Lyn, S. Einav, W. Rodi, and J.-H. Park, "A laser-Doppler velocimetry study of ensemble-averaged characteristics of the turbulent near wake of a square cylinder," *J. Fluid Mech.*, vol. 304, pp. 285–319, 1995.
[40] C. U. Buice, "Experimental investigation of flow through an asymmetric plane diffuser," 1997.
[41] C.-S. Song and S.-O. Park, "Numerical simulation of flow past a square cylinder using Partially-Averaged Navier–Stokes model," *J. Wind Eng. Ind. Aerodyn.*, vol. 97, no. 1, pp. 37–47, 2009.
[42] E. Jeong and S. S. Girimaji, "Partially Averaged Navier–Stokes (PANS) Method for Turbulence Simulations: Flow Past a Square Cylinder," *Journal of Fluids Engineering*, vol. 132, no. 12. pp. 1–11, 2010.